hydrogen

MDPI

Article

PdS-ZnS-Doped Electrospun Polymer Nanofibers as Effective Photocatalyst for Hydrogen Evolution

Gopal Panthi * and Arun Gyawali

School of Geomatics, Mid Baneshwor, P.O. Box 13177, Kathmandu 44618, Nepal
* Correspondence: gopalpanthi2003@gmail.com; Tel.: +977-1-4116177

Abstract: Poly(vinyl acetate) nanofibers doped with PdS-ZnS nanoparticles (PdS-ZnS/PVAc nanofibers) were fabricated via an electrospinning technique. PdS-ZnS nanoparticles were in situ synthesized by adding $(NH_4)_2S$ solution to poly(vinyl acetate)/zinc acetate/palladium acetate solution. Electrospinning of the formed colloidal solution led to the formation of poly(vinyl acetate) nanofibers containing uniformly distributed PdS-ZnS nanoparticles. The prepared samples were characterized by field emission scanning electron microscopy, X-ray diffraction, transmission electron microscopy and Fourier transform infrared spectroscopy. In photocatalytic activity investigation, the PdS-ZnS/PVAc nanofibers showed remarkably enhanced performance towards water photosplitting under solar irradiation compared to the ZnS/PVAc nanofibers. This enhanced performance is attributed to the synergistic effects of heterostructured PdS-ZnS nanoparticles, which can improve photogenerated charge migration and solar light absorption.

Keywords: electrospinning; composite nanofibers; ZnS; semiconductor; photocatalyst; water splitting; hydrogen evolution

Citation: Panthi, G.; Gyawali, A. PdS-ZnS-Doped Electrospun Polymer Nanofibers as Effective Photocatalyst for Hydrogen Evolution. *Hydrogen* **2024**, *5*, 403–413. https://doi.org/10.3390/hydrogen5030023

Academic Editor: Mohammed-Ibrahim Jamesh

Received: 7 June 2024
Revised: 1 July 2024
Accepted: 5 July 2024
Published: 7 July 2024

1. Introduction

The continuous use of fossil fuels to fulfill the social energy demands causes the emission of greenhouse effect gases, which are responsible for global warming and are a major concern for humanity. Therefore, world scientific communities are showing keen interest in searching for alternative and clean energy systems. Numerous efforts have been made for the eco-friendly production of hydrogen (H_2) as a pollution free and renewable energy [1,2]. In this regard, the evolution of hydrogen via photocatalytic water splitting using solar light-driven semiconductor photocatalysts has been regarded as the promising route to addressing the problem. Solar energy is a free, abundant and interminable source of energy, and its conversion into chemical energy causes zero pollution [3,4]. Semiconductor materials with a conduction band (CB) more negative than 0.0 eV and valence band (VB) more positive than 1.23 eV are considered active photocatalysts for water splitting under visible light irradiation. In general, the overall water splitting efficiency to evolve hydrogen utilizing semiconductor photocatalyst mainly depends on its light absorption capacity, VB/CB positions, charge transfer/separation efficiency and surface chemical reactions. Currently, various semiconductor photocatalysts are being applied for the evolution of hydrogen. Among these, metal sulfides, mainly ZnS and CdS, are considered emerging candidates for this purpose because of their appropriate bandgap, VB and CB positions and appropriate photocatalytic activity [5–7]. Particularly, ZnS is a widely studied semiconductor photocatalyst for hydrogen evolution because of its tendency to generate electron-hole pairs rapidly and the highly negative potential of excited electrons in the CB [8].

Furthermore, ZnS is a non-toxic, bio-safe and chemically stable II-IV type semiconductor with a bandgap of approximately 3.7 eV. The wide bandgap of ZnS limits its applications without coupling with narrow bandgap semiconductor cocatalysts. Therefore, coupling

a suitable cocatalyst with ZnS could be a good approach to promote its photostability. A suitable cocatalyst not only improves the active reaction sites and separation of photogenerated charge carriers, thereby suppressing their recombination but also decreases the activation potential of a photocatalyst for hydrogen evolution from an aqueous solution [9]. Owing to its adequate bandgap (1.6 eV) and higher optical absorption coefficient, PdS has been investigated as a cocatalyst for enhancing the photocatalytic hydrogen evolution activity of ZnS. PdS is a n-type semiconductor with a maximum absorption at c.a. λ = 650 nm visible range, and its incorporation with ZnS reduces the activation energy and fosters the oxidation-reduction reactions [10]. Moreover, the higher absorption coefficient of PdS allows it to function efficiently even at a small amount when incorporated with ZnS, thereby compensating for its relatively high cost. However, it would be better if future research was focused on finding the best alternatives to PdS, as Pd is a scarce and expensive element. To utilize the maximum advantages, PdS was chosen as a cocatalyst to introduce into ZnS for the elevation of its photocatalytic hydrogen evolution.

Electrospinning, a broadly recognized simple and versatile technique, has attracted growing attention for the fabrication of nanofibers from a polymer solution or melt using an electrostatic field. Nanofibers having a diameter ranging from 50 to 100 nm or greater can be fabricated utilizing this technique. The electrospun nanofibers possess unique properties like continuous morphology, high surface area, high porosity, flexibility and interconnectivity [11,12]. Importantly, these nanofiber properties are associated with the properties of electrospinning solution (viscosity, surface tension and conductivity), atmospheric conditions (temperature, pressure and humidity), applied voltage and tip-to-collector distance. Different types of nanofibers (polymeric, composite, carbon and ceramic) can be fabricated using this technique for diversified applications [13–16]. Additionally, electrospun nanofibers are mostly used as support materials for nanoparticles either by anchoring on the surface or encapsulating inside. These actions result in a uniform distribution of nanoparticles on/in nanofibers and can prevent the photocorrosion and agglomeration/loss of nanoparticles during large-scale applications [17,18].

Hence, considering the advantages of electrospun nanofibers and PdS as a cocatalyst to improve the photocatalytic performance of ZnS, this work reports a simple and facile strategy for fabricating PdS-ZnS/PVAc nanofibers following electrospinning technique. PdS was incorporated with ZnS nanoparticles by in situ precipitation route in PVAc solution. After electrospinning, PVAc nanofibers acted as a confined medium for uniformly distributed PdS-ZnS composite nanoparticles. Fabricated composite nanofibers exhibited high photocatalytic stability for evolving hydrogen from water splitting, solar light-driven activity and better reusability. Also, this fabrication strategy could be an effective remedy for handling and separating photocatalyst.

2. Materials and Methods

2.1. Chemicals

Poly(vinyl acetate) (PVAc, MW 5,500,000 g/mol), zinc acetate dihydrate (ZnAc), palladium acetate (PdAc, reagent grade 98%), ammonium sulfide [$(NH_4)_2S$ 40–48 wt% solution in water], sodium sulfide (Na_2S) and sodium sulfite (Na_2SO_3) were purchased from Sigma-Aldrich, St. Louis, MO, USA. N,N-dimethylformamide (DMF) was purchased from Daejung Chemicals, South Korea. All the chemicals were of AR grade and used without further treatment. Distilled water was used to prepare aqueous solutions.

2.2. Fabrication of PdS-ZnS/PVAc Nanofibers

In a typical procedure, 18 wt% of PVAc solution was prepared by dissolving in DMF under magnetic stirring (first solution). Similarly, 0.5 g of ZnAc and 0.125 g of PdAc were separately dissolved in 1 mL of DMF. These two salt solutions were mixed together (second solution). Then, the second solution was mixed with 5 mL of 18 wt% of PVAc solution under constant stirring for 2 h (third solution). The final colloidal solution was prepared by dropping 0.5 mL of $(NH_4)_2S$ solution into the third solution under vigorous

stirring to achieve good dispersion of PdS-ZnS nanoparticles in the solution, which was left under continuous stirring for another 5 h. After, the colloidal solution was subjected to electrospinning using a high voltage of 15 kV. In the electrospinning process, the solution was fed to 5 mL syringe provided with a plastic micro-tip placed 15 cm apart from rotating drum collector. The developing PdS-ZnS/PVAc nanofibers were collected on the drum collector rotating with a constant speed by DC motor. After vacuum drying for 24 h, the as-fabricated PdS-ZnS/PVAc electrospun nanofiber mat was used for further analysis. For comparison, pure PVAc and ZnS/PVAc electrospun nanofiber mats were also prepared following same procedure without adding ZnAc/PdAc and PdAc, respectively. The schematic for the fabrication of PdS-ZnS/PVAc electrospun nanofibers is illustrated in Figure 1.

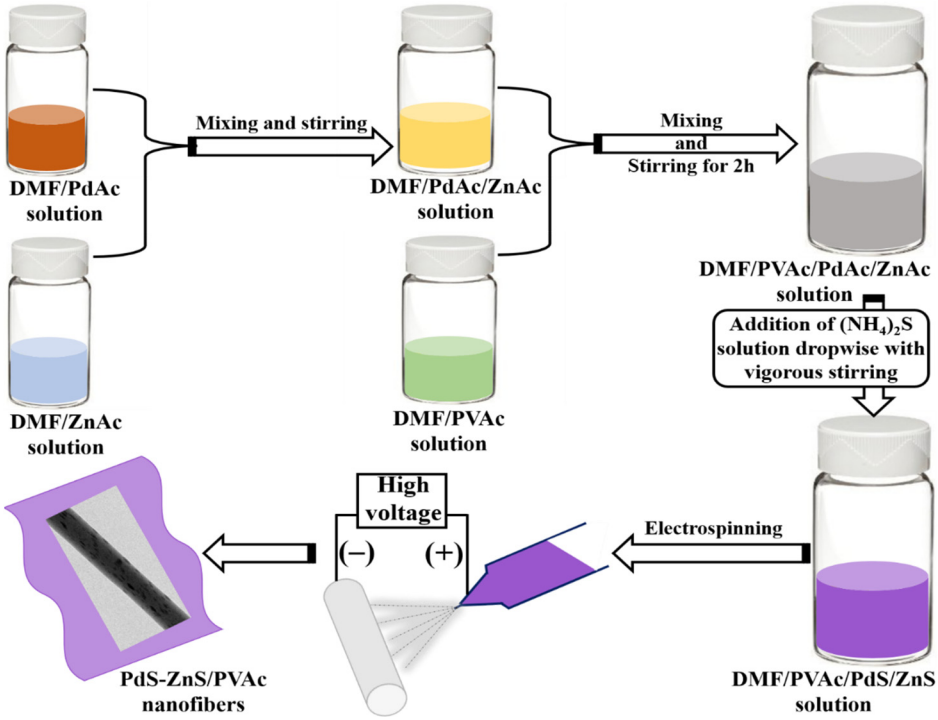

Figure 1. Schematic illustration for the fabrication of PdS-ZnS/PVAc nanofibers.

2.3. Characterization

Surface morphology of electrospun nanofibers was characterized by field emission scanning electron microscope (FESEM, S-7400, Hitachi, Tokyo, Japan) provided with energy dispersive X-ray spectroscopy (EDS).Composition of samples was studied using EDS. Information regarding phase and crystallinity of the samples was obtained with X-ray diffractometer (XRD, Rigaku, Tokyo, Japan) with Kα (λ = 1.540 Å) radiation over Bragg angles ranging from 10° to 80°. Furthermore, distribution of nanoparticles in PVAc nanofibers was observed using transmission electron microscope (TEM, JEM-2010, JEOL, Tokyo, Japan) with a 200 kV accelerating voltage, and the perfectly crystalline nature of nanoparticles was identified from high-resolution TEM (HR-TEM) images. For TEM/HR-TEM microscopy, the samples were prepared by collecting nanofibers on TEM grid during electrospinning. Fourier transform infrared (FTIR) spectroscopy (FT-IR, FT/IR-4200, Tokyo, Japan) was applied to analyze the bonding configuration of nanoparticles with PVAc.

2.4. Photocatalytic Water Splitting for Hydrogen Evolution

Photocatalytic water splitting experiment utilizing ZnS/PVAc and PdS-ZnS/PVAc nanofiber mats was conducted in a natural atmospheric condition on a sunny day under uninterrupted sunlight (from 11 a.m. to 3.30 p.m.). The solar radiation was measured using a solar power meter TM-206 (TENMARS ELECTRONICS, Taipei, Taiwan). The average

amount of solar radiation (radiation flux per unit area) was measured to be 16.25 MJ/m^2. In this experiment, the rate of hydrogen generation was measured in a typical water-filled graduated cylinder. The graduated cylinder filled with water was connected to the reaction flask (placed on magnetic stirrer) using flexible pipe to measure the volume of hydrogen gas that evolved from the reaction. A weighed amount (140 mg) of each nanofiber mat was added into the reaction flask containing 200 mL of aqueous solution of Na_2S (0.5 M) and Na_2SO_3 (0.5 M) as sacrificial agents. The volume of hydrogen gas evolved in presence of solar irradiation under constant magnetic stirring was measured by recording the displacement of water in graduated cylinder every 25 min. Finally, the reaction ended when no hydrogen gas generation was observed. Then, the exact volume of dry hydrogen at normal temperature and pressure (NTP) was obtained from combined gas equations in which ambient temperature and pressure were also considered. Schematic illustration of the evolution of hydrogen gas from photosplitting of water is shown in Figure 2.

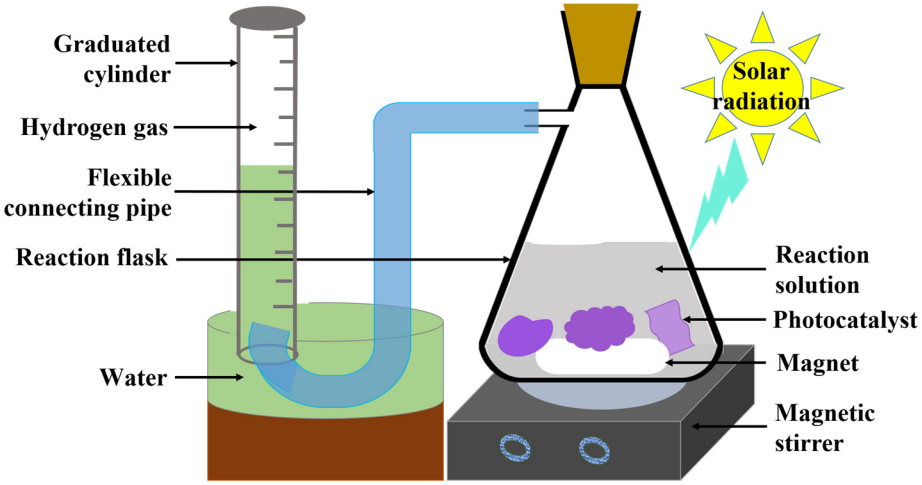

Figure 2. Schematic illustration for the evolution of hydrogen gas from photosplitting of water. Photocatalyst = PdS-ZnS/PVAc nanofiber mat; reaction solution = solution of water, Na_2S and Na_2SO_3.

3. Results and Discussion

The surface morphology of as-fabricated nanofibers was studied using FESEM characterization (Figure 3a–c). All formulations exhibited continuous, randomly oriented and bead-free smooth nanofibers. It was observed that in situ synthesis of PdS and ZnS nanoparticles did not affect the nanofiber morphology. Also, the absence of nanoparticles on the surface of composite nanofibers was confirmed by FESEM images (Figure 3b,c). In addition, compared to pure PVAc nanofibers (Figure 3a), the diameter of ZnS/PVAc nanofibers (Figure 3b) and PdS-ZnS/PVAc nanofibers (Figure 3c) was observed to be slightly decreased (ranging from 200 nm to 300 nm). The result signified that the addition of nanoparticles led to a decrease in fiber diameter. This could be ascribed to the increase in electrical conductivity of colloidal polymer solution that resulted in the formation of even more uniform nanofibers with thinner diameters [19,20].

Moreover, FESEM-EDS spectra of PdS-ZnS/PVAc nanofibers (Figure 3d) revealed the presence of Zn, S and Pd elements in PVAc nanofibers without other impurity elements. Similarly, the spatial distribution of Zn, Pd and S in PVAc nanofibers was examined by elemental mapping of PdS-ZnS/PVAc nanofibers (Figure 4). As depicted in the Figure, these elements are seen homogeneously distributed in the nanofibers, confirming the existence of PdS-ZnS nanoparticles.

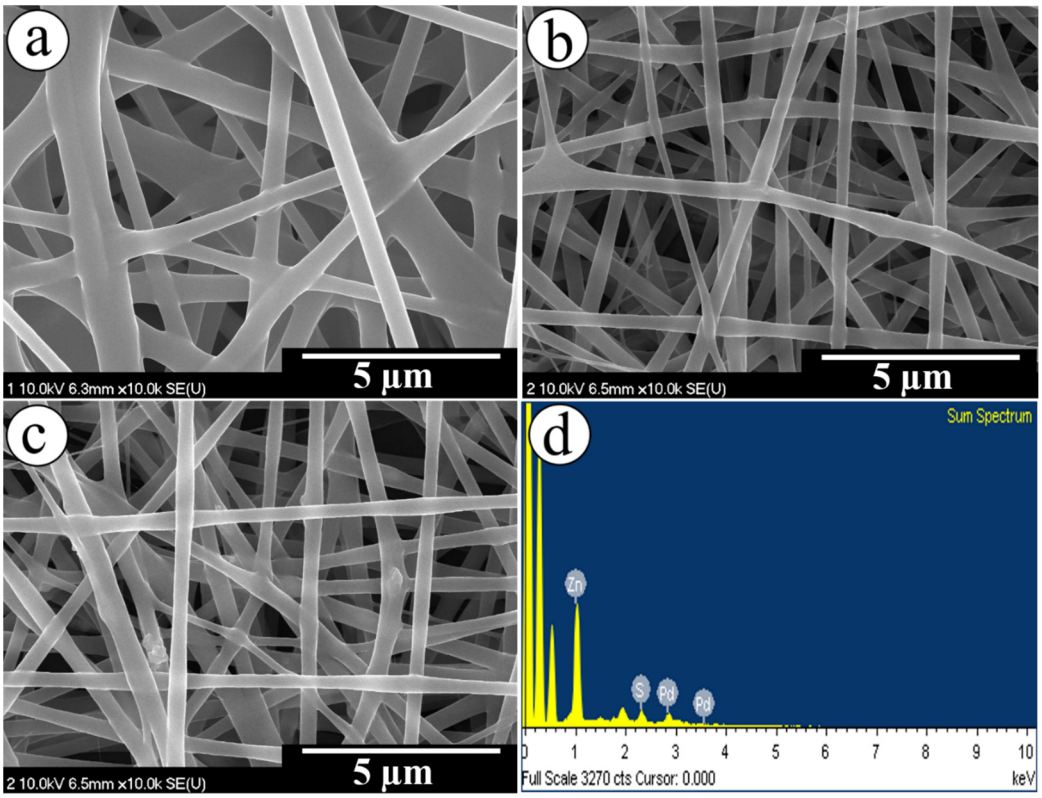

Figure 3. FESEM images; (**a**) pure PVAc nanofibers, (**b**) ZnS/PVAc nanofibers, (**c**) PdS-ZnS/PVAc nanofibers and (**d**) EDS of PdS-ZnS/PVAc nanofibers.

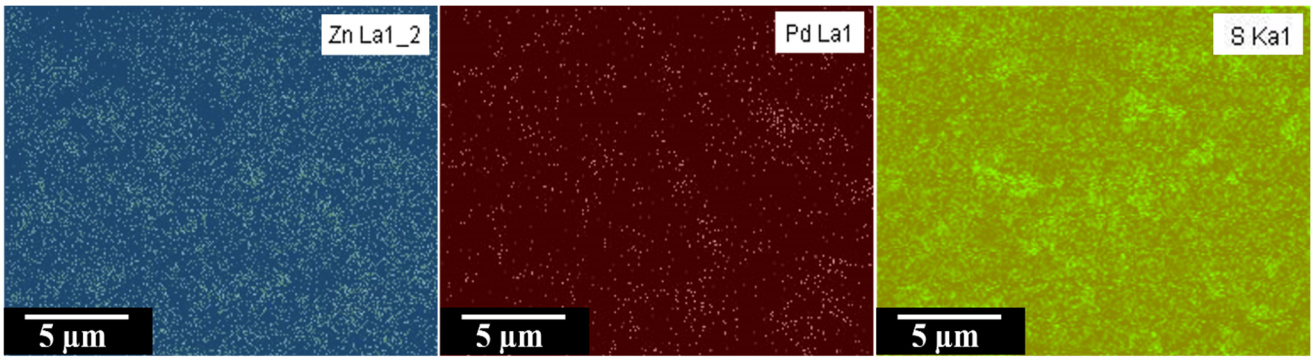

Figure 4. Elemental mapping of PdS-ZnS/PVAc nanofibers.

In order to study the crystalline nature of different samples, XRD analysis was performed. The XRD diffraction patterns of the PdS-ZnS/PVAc nanofiber mat compared with pure PVAc nanofiber mat and ZnS/PVAc nanofiber mat are shown in Figure 5. The broad peak with low crystallinity centered at around 2θ of 20° in all formulations was assigned to PVAc polymer. Besides, the sharp peaks centered at 2θ of 28.68° and 56.47° in the diffraction patterns of ZnS/PVAc nanofibers and PdS-ZnS/PVAc nanofibers were assigned to the (111) and (311) crystallographic planes of ZnS, respectively (JCPDS No. 772100) [9]. It is worth noting that no characteristic peaks associated with PdS were observed in PdS-ZnS/PVAc nanofibers, which may be ascribed to the low amount of PdS to be identified by XRD. However, the presence of Pd in the composite nanofibers was confirmed by FESEM-EDS (Figure 3d) and image mapping (Figure 4). Additionally, no peaks belonging to any other phase were detected.

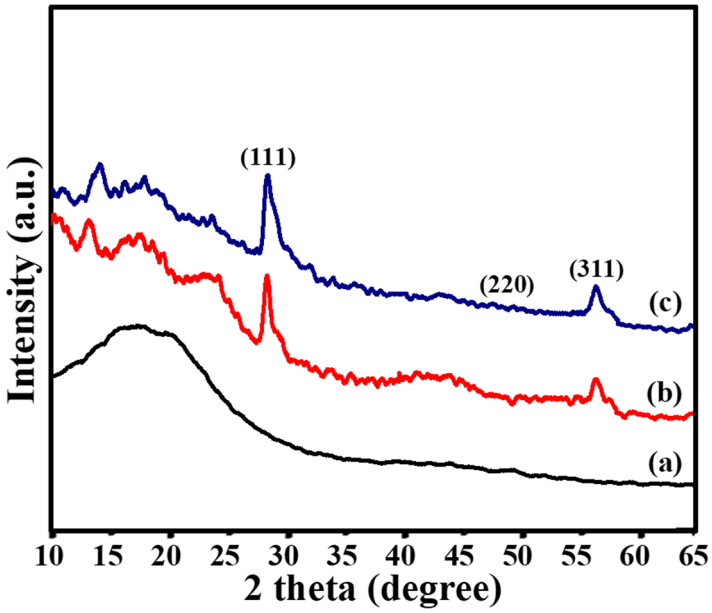

Figure 5. XRD diffraction patterns; (a) pure PVAc nanofibers; (b) ZnS/PVAc nanofibers and (c) PdS-ZnS/PVAc nanofibers.

Figure 6 illustrates the TEM image of PVAc nanofiber (Figure 6a), ZnS/PVAc nanofiber (Figure 6b) and Pds-ZnS/PVAc nanofiber (Figure 6c). Likewise, Figure 6d illustrates the HR-TEM image of PdS-ZnS nanoparticles. Compared to pure PVAc nanofiber, ZnS/PVAc and Pds-ZnS/PVAc nanofibers showed highly dispersed and mostly rice grain-shaped nanoparticles inside the polymer nanofiber. In both samples, the size of nanoparticles was in the range of 5–10 nm. Such nanoparticles in non-aggregated form possess a large surface area and, thus, are beneficial for chemical and physical functionalities. It is reported that the immobilization of nanoparticles inside the polymer nanofiber is due to the smaller size of nanoparticles than that of nanofibers [21]. Moreover, a homogeneous distribution of nanoparticles inside the nanofibers might be obtained due to Coulombic repulsion between charged Pd^{2+} and Zn^{2+} nanoparticles during electrospinning. Accordingly, polycrystalline PdS-ZnS composite nanoparticles were observed in the HR-TEM image in which the lattice fringes with a planar spacing of 0.23 nm and 0.32 nm represent the interplanar distance to PdS (202) and ZnS (111), respectively [22,23]. Importantly, no amorphous phases between PdS and ZnS were observed, which indicated the formation of atomic heterojunctions. As reported in reference [24], the formation of heterojunction would favor the migration of photogenerated electrons and holes across the PdS-ZnS interface and consequently prevent their recombination. Hence, the results obtained from FESEM-EDS, image mapping and TEM/HR-TEM indicated successful fabrication of Pds-ZnS/PVAc composite nanofibers.

FTIR spectra of pure PVAc, ZnS/PVAc and PdS-ZnS/PVAc nanofibers are presented in Figure 7. As shown, all formulations display characteristic peaks at 1739.4 cm^{-1} ($\upsilon_{C=O}$), 1239.9 and 1020.9 cm^{-1} (υ_{C-O}) and 1375.7 cm^{-1} (δ_{CH3}) corresponding to PVAc polymer (Sprouse collection of IR, card no. 187–189) [25]. The ZnS/PVAc and PdS-ZnS/PVAc composite nanofibers also showed the same spectra of PVAc with some reduced intensity, which might be due to the loading of nanoparticles in PVAc nanofibers. Therefore, it is concluded that the chemical structure of PVAc polymer was not influenced by the proposed synthesis strategy.

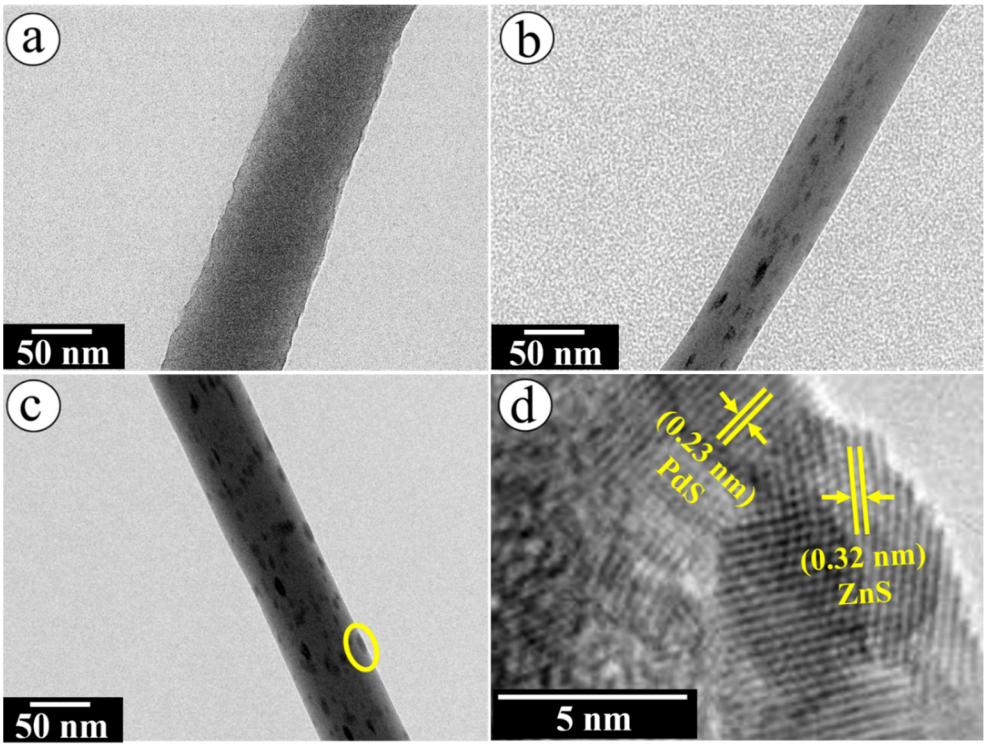

Figure 6. TEM images: (**a**) pure PVAc nanofiber, (**b**) ZnS/PVAc nanofiber and (**c**) PdS-ZnS/PVAc nanofiber with yellow circled area selected for the HR-TEM analysis. Panel (**d**) represents the HR-TEM image from yellow circled area of (**c**).

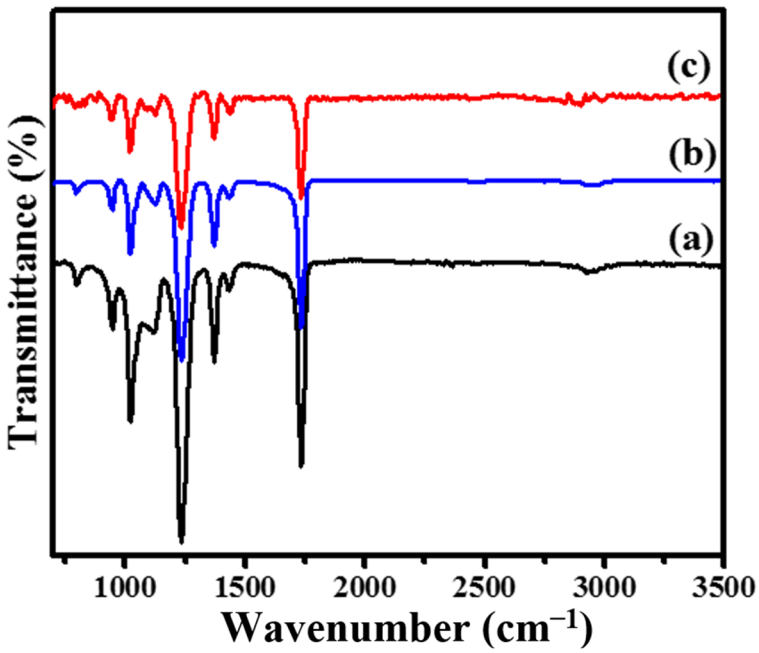

Figure 7. FTIR spectra: (a) pure PVAc nanofibers, (b) ZnS/PVAc nanofibers and (c) PdS-ZnS/PVAc nanofibers.

Results of photocatalytic performance exhibited by ZnS/PVAc nanofibers and PdS-ZnS/PVAc nanofibers for the photosplitting of water in the presence of Na_2S and Na_2SO_3 to evolve hydrogen under solar irradiation are presented in Figure 8. As shown, both the samples revealed good photocatalytic performance; however, PdS-ZnS/PVAc nanofibers showed higher performance for the evolution of hydrogen (1.19 mmol) compared to the

ZnS/PVAc nanofibers (0.74 mmol) within the observed time of 250 min. Additionally, the cycling experiment of used PdS-ZnS/PVAc nanofibers under similar conditions showed good stability in the second cycle, but there was slightly decreased performance, which could be due to the loss of photocatalyst during the separation process. It is inferred that the enhanced performance of PdS-ZnS/PVAc nanofibers is associated with the loading of low bandgap PdS as cocatalyst on ZnS nanoparticles so that (i) the solar light absorption ability of PdS-ZnS heterostructured nanoparticles increased through lowering the bandgap and (ii) the heterojunction formed between PdS and ZnS nanoparticles favored the migration of photogenerated charge carriers across the PdS-ZnS interface and, consequently, suppressed their recombination. Interestingly, due to the presence of methyl groups, PVAc polymer possesses good electrical conductivity [26]. Therefore, PVAc not only served as nanoparticle carriers but also played an important role in the photocatalytic process rather than affecting it. Covering PdS-ZnS nanoparticles with PVAc created a network of conducting layers around the nanoparticles, which could promote the generation/migration of photogenerated charge carriers. and prevent their recombination.

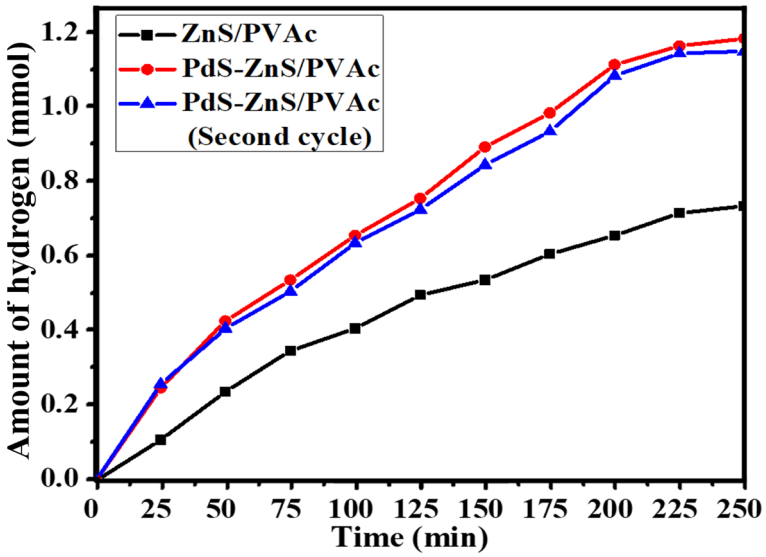

Figure 8. Reaction time course of hydrogen evolution under solar irradiation.

Based on the reported bandgap positions of PdS and ZnS, the mechanism of water photosplitting for hydrogen evolution utilizing PdS-Zn/PVAc nanofibers has been proposed. The reported VB and CB positions of PdS are +1.34 V and −0.26 V vs. NHE (normal hydrogen electrode), respectively [23,27,28]. Similarly, the reported VB and CB positions of ZnS are −0.91 V and +2.44 vs. NHE, respectively [29,30]. Under solar irradiation, photogenerated electrons and holes are generated in the CB and VB of ZnS, respectively. Since the VB position of PdS (+1.34 V vs. NHE) is less positive than that of ZnS (+2.44 V vs. NHE), the photogenerated holes from the VB of ZnS are transferred to the VB of PdS. Hence, PdS itself couldnot exhibit photocatalytic hydrogen evolution but it acted as a cocatalyst with ZnS for accepting photogenerated holes from ZnS and enhancing the preferred separation of photogenerated electrons and holes. PdS, as an oxidation cocatalyst, oxidizes sulfide (S^{2-}) and sulfite (SO_3^{2-}) ions of sacrificial agents to degraded products thiosulfate ($S_2O_3^{2-}$) and sulfate (SO_4^{2-}) ions. It is suggested that the use of S^{2-} and SO_3^{2-} as sacrificial agents can inhibit the formation of disulfide ions and enhance the evolution of hydrogen from water splitting [31]. The role of PdS as an oxidation cocatalyst has also been reported in previous reports [30,32–34]. Additionally, the conductive network of PVAc promoted the generation of photogenerated charge carriers, enhanced the migration of photogenerated holes from ZnS to PdS and prevented their recombination. In the meantime, the photogenerated electrons in the CB of ZnS are captured by H^+, resulting in the formation of H_2, since the CB of ZnS is sufficiently negative to generate H_2 by reducing water [0 V vs. NHE; H^+/H_2].

The schematic of the proposed charge transfer mechanism on PdS-ZnS/PVAc nanofibers photocatalyst is illustrated in Figure 9. The possible photochemical reactions taking place in water splitting for the evolution of H_2 in the $S^2/SO_3{}^{2-}$ system are summarized in the following Equations (1)–(6).

$$2H_2O + \left(2e^-_{CB}\right) \rightarrow H_2 + 2OH^- \quad (1)$$

$$SO_3^{2-} + 2OH^- + \left(2h^+_{VB}\right) \rightarrow SO_4^{2-} + H_2O \quad (2)$$

$$2SO_3^{2-} + 2h^+ \rightarrow S_2O_6^{2-} \quad (3)$$

$$2S^{2-} + 2h^+ \rightarrow S_2^{2-} \quad (4)$$

$$SO_3^{2-} + S^{2-} + 2h^+ \rightarrow S_2O_3^{2-} \quad (5)$$

$$SO_3^{2-} + S_2^{2-} \rightarrow S_2O_3^{2-} + S^{2-} \quad (6)$$

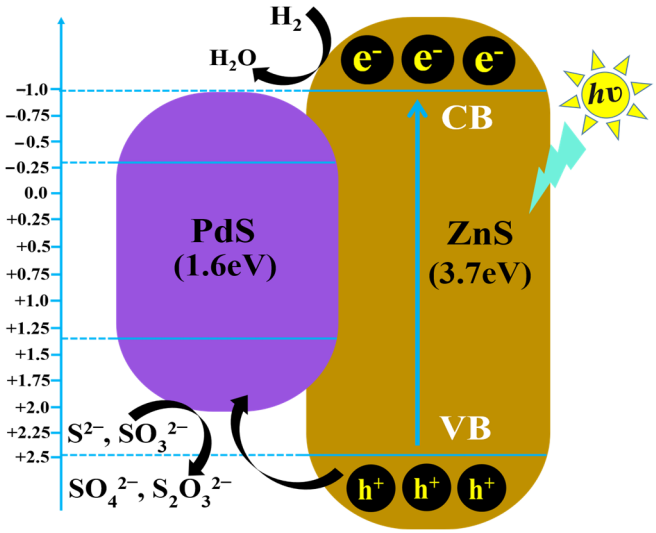

Figure 9. Schematic illustration of proposed charge transfer mechanism on PdS-ZnS/PVAc nanofibers photocatalyst.

4. Conclusions

In summary, PdS-ZnS/PVAc nanofibers were successfully fabricated by chemical synthesis and electrospinning techniques. FESEM and TEM characterizations revealed that the in situ synthesized PdS-ZnS nanoparticles were well dispersed in PVAc nanofibers. The photocatalytic hydrogen evolution activity of PdS-ZnS/PVAc nanofibers was determined by water splitting in the presence of Na_2S and Na_2SO_3 as sacrificial agents under solar irradiation. Compared to ZnS/PVAc nanofibers, PdS-ZnS/PVAc nanofibers were found to be superior for hydrogen evolution (1.19 mmol) within 250 min, which can be ascribed to the loading of PdS as cocatalyst on ZnS nanoparticles. We also conclude with the finding that the loading of a cocatalyst (PdS) with a low bandgap could play important roles in improving the separation of photogenerated charge carriers and increasing the solar light absorption efficiency through narrowing ZnS bandgap. Finally, this work may provide a new avenue to design and fabricate composite nanofibers having bi-component metal sulfide nanoparticles uniformly distributed inside the polymer nanofibers for improving hydrogen production activity from solar water photosplitting. Also, this synthesis strategy prevents the nanoparticles from loss and agglomeration, which eventually makes the separation process easier.

Author Contributions: For this research article, the individual contributions of the authors were as follows: conceptualization, G.P.; methodology, G.P.; software, G.P.; validation, G.P. and A.G.; formal analysis, G.P.; investigation, G.P. and A.G.; resources, A.G.; data curation, G.P.; writing—original draft preparation, G.P.; writing—review and editing, G.P. and A.G.; visualization, A.G.; supervision, G.P.; project administration, A.G.; funding acquisition, A.G. All authors have read and agreed to the published version of the manuscript.

Funding: This research work was supported by the School of Geomatics research grant (F.Y. 2080/81).

Data Availability Statement: The original contributions presented in the study are included in the article, further inquiries can be directed to the corresponding author.

Acknowledgments: We are grateful to program coordinator Pushpa Thapa and Damodar Gautam of the School of Geomatics for providing valuable administrative and technical support to carry out this research work.

Conflicts of Interest: The authors declare no conflicts of interest.

References

1. Chen, S.; Wang, W.; Hou, Y.; Hao, Y.; Zhao, Y.; Wang, S.; Meng, J.; Xu, H. Co_3O_4 nanosheet/g-C_3N_4 hybrid photocatalysts for promoted H_2 evolution. *ACS Appl. Nano Mater.* **2023**, *6*, 8717–8725. [CrossRef]
2. Zhao, F.; Zhang, M.; Yan, D.; Hu, X.; Fan, J.; Sun, T.; Liu, E. S-scheme Co_9S_8 nanoflower/red phosphorus nanosheet heterojunctions for enhanced photocatalytic H_2 evolution. *ACS Appl. Nano Mater.* **2023**, *6*, 14478–14487. [CrossRef]
3. Lange, T.; Reichenberger, S.; Ristig, S.; Rohe, M.; Strunk, J.; Barcikowski, S.; Schlögl, R. Zinc sulfide for photocatalysis: White angel or black sheep? *Prog. Mater. Sci.* **2022**, *124*, 100865. [CrossRef]
4. Dong, J.; Fang, W.; Hui, Y.; Xia, W.; Zeng, X.; Shangguan, W. Few-layered MoS_2/ZnCdS/ZnS heterostructures with an enhanced photocatalytic hydrogen evolution. *ACS Appl. Energy Mater.* **2022**, *5*, 4893–4902. [CrossRef]
5. Wu, P.; Liu, H.; Xie, Z.; Xie, L.; Liu, G.; Xu, Y.; Chen, J.; Lu, C.Z. Excellent charge separation of NCQDs/ZnS nanocomposites for the promotion of photocatalytic H_2 evolution. *ACS Appl. Mater. Interfaces* **2024**, *16*, 16601–16611. [CrossRef]
6. Huang, H.; Dai, B.; Wang, W.; Lu, C.; Kou, J.; Ni, Y.; Wang, L.; Xu, Z. Oriented built-in electric field introduced by surface gradient diffusion doping for enhanced photocatalytic H2 evolution in CdS nanorods. *Nano Lett.* **2017**, *17*, 3803–3808. [CrossRef] [PubMed]
7. Yang, Y.; Peng, S.; Han, Z.; Fu, M.; Wang, K.; Yu, H. CdS Nanorods with an Optimized ZnS Coating as Composite Photocatalysts for Enhanced Water Splitting under Solar Light Irradiation. *ACS Appl. Nano Mater.* **2022**, *5*, 9747–9753. [CrossRef]
8. Hong, E.; Kim, D.; Kim, J.H. Heterostructured metal sulfide (ZnS-CuS-CdS) photocatalyst for high electron utilization in hydrogen production from solar water splitting. *J. Ind. Eng. Chem.* **2014**, *20*, 3869–3874. [CrossRef]
9. Arun Kumar, G.; Bhojya Naik, H.S.; Viswanath, R.; Suresh Gowda, I.K.; Santosh, K.N. Tunable emission property of biotin capped Gd:ZnS nanoparticles and their antibacterial activity. *Mater. Sci. Semicond. Process.* **2017**, *58*, 22–29. [CrossRef]
10. Mao, S.; Shi, J.W.; Sun, G.; Zhang, Y.; Ma, D.; Song, K.; Lv, Y.; Zhou, J.; Wang, H.; Cheng, Y. PdS quantum dots as a hole attractor encapsulated into the MOF@$Cd_{0.5}Zn_{0.5}S$ heterostructure for boosting photocatalytic hydrogen evolution under visible light. *ACS Appl. Mater. Interfaces* **2022**, *14*, 48770–48779. [CrossRef]
11. Panthi, G.; Barakat, N.A.M.; Risal, P.; Yousef, A.; Pant, B.; Unnithan, A.R.; Kim, H.Y. Preparation and characterization of nylon-6/gelatin composite nanofibers via electrospinning for biomedical applications. *Fibers Polym.* **2013**, *14*, 718–723. [CrossRef]
12. Babazadeh-Mamaqani, M.; Razzaghi, D.; Roghani-Mamaqani, H.; Babie, A.; Rezaei, M.; Hoogenboom, R.; Salami-Kalajahi, M. Photo-responsive electrospun polymer nanofibers: Mechanisms, properties, and applications. *Prog. Mater. Sci.* **2024**, *146*, 101312. [CrossRef]
13. Wang, X.X.; Yu, G.F.; Zhang, J.; Yu, M.; Ramakrishna, S.; Long, Y.Z. Conductive polymer ultrafine fibers via electrospinning: Preparation, physical properties and applications. *Prog. Mater. Sci.* **2021**, *115*, 100704. [CrossRef]
14. Panthi, G.; Park, S.-J.; Kim, T.-W.; Chung, H.-J.; Hong, S.-T.; Park, M.; Kim, H.-Y. Electrospun composite nanofibers of polyacrylonitrile and Ag2CO3 nanoparticles for visible light photocatalysis and antibacterial applications. *J. Mater. Sci.* **2015**, *50*, 4477–4485. [CrossRef]
15. Chen, S.; Qiu, L.; Cheng, H.M. Carbon-based fibers for advanced electrochemical energy storage devices. *Chem. Rev.* **2020**, *120*, 2811–2878. [CrossRef] [PubMed]
16. Panthi, G.; Park, S.J.; Chung, H.J.; Park, M.; Kim, H.Y. Silver nanoparticles decorated Mn_2O_3 hybrid nanofibers via electrospinning; towards the development of new bactericides with synergistic effect. *Chem. Phys.* **2017**, *189*, 70–75. [CrossRef]
17. Panthi, G.; Gyawali, K.R.; Park, M. Towards the enhancement in photocatalytic performance of Ag_3PO_4 nanoparticles through sulfate doping and anchoring on electrospun nanofibers. *Nanomaterials* **2020**, *10*, 929. [CrossRef] [PubMed]
18. Quilez-Molina, A.I.; Barroso-Solares, S.; Hurtado-Garcia, V.; Heredia-Guerrero, J.A.; Rodriguez-Mendez, M.L.; Rodriguez-Perez, M.A.; Pinto, J. Encapsulation of copper nanoparticles in electrospun nanofibers for sustainable removal of pesticides. *ACS Appl. Mater. Interfaces* **2023**, *15*, 20385–20397. [CrossRef] [PubMed]
19. Zhang, H.; Xia, J.; Pang, X.; Zhao, M.; Wang, B.; Yang, L.; Wan, H.; Wu, J.; Fu, S. Magnetic nanoparticle-loaded electrospun polymeric nanofibers for tissue engineering. *Mater. Sci. Eng. C* **2017**, *73*, 537–543. [CrossRef]

20. Nkabinde, S.C.; Moloto, M.J.; Matabola, K. Optimized loading of TiO_2 nanoparticles into electrospun polyacrylonitrile and cellulose acetate polymer fibers. *J. Nanomater.* **2020**, *1*, 9429421. [CrossRef]
21. Barakat, N.A.M.; Abadir, M.F.; Sheikh, F.A.; Kanjwal, M.A.; Park, S.J.; Kim, H.Y. Polymeric nanofibers containing solid nanoparticles prepared by electrospinning and their applications. *Chem. Eng. J.* **2010**, *156*, 487–495. [CrossRef]
22. Ma, L.; Lin, C.; Jiang, W.; Yan, S.; Jiang, H.; Song, X.; Ai, X.; Cao, X.; Ding, Y. Achieving highly efficient photocatalytic hydrogen evolution through the construction of g-C_3N_4@PdS@Pt nanocomposites. *Molecules* **2024**, *29*, 493. [CrossRef]
23. Liu, S.; Wang, X.; Wang, K.; Lv, R.; Xu, Y. ZnO/ZnS-PdS core/shell nanorods: Synthesis, characterization and application for photocatalytic hydrogen production from a glycerol/water solution. *Appl. Surf. Sci.* **2013**, *283*, 732–739. [CrossRef]
24. Yang, J.H.; Yan, H.J.; Wang, Z.L.; Wen, F.Y.; Wang, Z.J.; Fan, D.Y.; Shi, J.Y.; Li, C. Roles of cocatalysts in Pt–PdS/CdS with exceptionally high quantum efficiency for photocatalytic hydrogen production. *J. Catal.* **2012**, *290*, 151–157. [CrossRef]
25. Zeng, J.; Yang, J.; Zhu, Y.; Liu, Y.; Qian, Y.; Zheng, H. Nanocomposite CdS particles in polymer rods fabricated by a novel hydrothermal polymerization and simultaneous sulfidation technique. *Chem. Commun.* **2001**, *17*, 1332–1333. [CrossRef]
26. Panthi, G.; Ranjit, R.; Khadka, S.; Gyawali, K.R.; Kim, H.Y.; Park, M. Characterization and antibacterial activity of rice grain-shaped ZnZ nanoparticles immobilized inside the polymer electrospun nanofibers. *Adv. Compos. Hybrid Mater.* **2020**, *3*, 8–15. [CrossRef]
27. Barawi, M.; Ferrer, I.J.; Ares, J.R.; Sanchez, C. Hydrogen Evolution Using Palladium Sulfide (PdS) Nanocorals as Photoanodes in Aqueous Solution. *ACS Appl. Mater. Interfaces* **2014**, *6*, 20544–20549. [CrossRef] [PubMed]
28. Li, X.J.; Qi, M.Y.; Li, J.Y.; Tan, C.L.; Tang, Z.R.; Xu, Y.J. Visible light driven dehydrocoupling of thiols to disulfides and evolution over PdS-decorated $ZnInS_4$ composites. *Chin. J. Catal.* **2023**, *51*, 5565. [CrossRef]
29. Zhang, J.; Yu, J.; Zhang, Y.; Li, Q.; Gong, J.R. Visible Light Photocatalytic H_2-Production Activity of CuS/ZnS Porous Nanosheets Based on Photoinduced Interfacial Charge Transfer. *Nano Lett.* **2011**, *11*, 4774–4779. [CrossRef] [PubMed]
30. Meng, J.; Yu, Z.; Li, Y.; Li, Y. PdS-modified CdS/NiS composite as an efficient photocatalyst for H_2 evolution in visible light. *Catal. Today* **2013**, *225*, 136–141. [CrossRef]
31. Schneider, J.; Bahnemann, D.W. Undesired role of sacrificial reagents in photocatalysis. *J. Phys. Chem. Lett.* **2013**, *4*, 3479–3483. [CrossRef]
32. Yan, H.J.; Yang, J.H.; Ma, G.J.; Wua, G.P.; Zong, X.; Lei, Z.B.; Shi, J.Y.; Li, C. Visible-light-driven hydrogen production with extremely high quantum efficiency on Pt-PdS/CdS photocatalys. *J. Catal.* **2009**, *266*, 165–168. [CrossRef]
33. Khan, K.; Tao, X.; Zhao, Y.; Zeng, B.; Shi, M.; Ta, N.; Li, J.; Jin, J.; Li, R.; Li, C. Spatial separation of dual-cocatalysts on one-dimensional semiconductors for photocatalytic hydrogen production. *J. Mater. Chem. A* **2019**, *7*, 15607–15614. [CrossRef]
34. Chen, Q.; Suo, C.; Zhang, S.; Wang, Y. Effect of PdS on Photocatalytic Hydrogen Evolution of Nanostructured CdS under Visible Light Irradiation. *Int. J. Photoenergy* **2013**, *1*, 149586. [CrossRef]